Hydrology and Earth System Sciences Discussions

Uncertainties in using remote sensing for water use determination: a case study in a heterogeneous study area in South Africa

L. A. Gibson[1,2], Z. Münch[3], J. Engelbrecht[4], and J. E. Conrad[5]

[1]Agricultural Research Council-Institute for Soil, Climate and Water, Private Bag X5017, Stellenbosch, 7599, South Africa
[2]Department of Environmental and Geographical Science, University of Cape Town, Shell Environmental & Geographical Science Building, South Lane, Upper Campus, University of Cape Town, Private Bag X3, Rondebosch 7701, South Africa
[3]Stellenbosch University, Private Bag X1, Matieland, 7602, South Africa
[4]Council for Geoscience, Western Cape Unit, P.O. Box 572, Bellville, 7535, South Africa

---

Title Page

Abstract	Introduction
Conclusions	References
Tables	Figures

|◄ | ►|

◄ | ►

Back | Close

Full Screen / Esc

Printer-friendly Version

Interactive Discussion

[5]GEOSS – Geohydrological and Spatial Solutions International (Pty) Ltd, P.O. Box 12412, Die Board, 7613, South Africa

Correspondence to: L. A. Gibson (gibsonl@arc.agric.za)

Full Screen / Esc

Printer-friendly Version

Interactive Discussion

Abstract

South Africa is a water scarce country where it is important for water managers to have accurate information on water resource occurrence and use. A remote sensing project highlighted many uncertainties in using complex remote sensing models to determine water use in a heterogeneous study area. The severity of the uncertainties was con-firmed as the results across the catchment showed a higher total evapotranspiration than precipitation. This paper illustrates some of the uncertainties and limitations using the evapotranspiration component of the water balance as calculated by the Surface Energy Balance System (SEBS) model, as an example.

The introduction of uncertainties in the derivation of evapotranspiration were identi-fied as: (1) sensitivity to land surface and air temperature gradient; (2) the choice of fractional vegetation cover formula; (3) height of wind speed measurement in relation to displacement height indicating a maximum canopy height at which the SEBS model should be used; and (4) study area heterogeneity.

Uncertainties and errors are compounded when considering that the SEBS model is a complex model, requiring several image processing sequences that are combined to produce the final result. It was shown how the production and propagation of errors in the SEBS model can contribute to uncertainties in flux estimation and ultimately to uncertainties in the estimation of actual evapotranspiration.

1 Introduction

The pressure on water resources in South Africa creates a need for water resource managers to have accurate information on all aspects of water resource occurrence and use. To quantify the various components involved in calculating water use by means of field-based observations would be a difficult and time consuming process, providing only point-based measurements at a specific point in time. This problem is compounded when one considers that several measurements over time would be

needed to accurately measure or monitor water use. To address these problems, Gibson et al. (2010) investigated the usefulness and applicability of remote sensing technologies as a tool for water resource assessment and specifically for the quantification of water use at farm level. Their approach relied on a simplified equation in which each
5 component of the water balance equation was calculated for a hydrological year using mostly remote sensing techniques or products where possible.

To derive these datasets several complex models were applied to the input data. Although all of the components quantified by remote sensing data were subject to uncertainties and limitations, Gibson et al. (2010) were alerted to the possibility of
10 uncertainties through the calculation of evapotranspiration (ET). The calculation of ET revealed that the total annual ET calculated using the Surface Energy Balance System (SEBS) model for the study area exceeded the total rainfall for the same area and time period. As a consequence, the origins of uncertainties with regard to the accuracy of the final results were explored using the estimation of ET as an example.
15 The derivation of ET is a complex process requiring several sources of input data and several processing steps to derive intermediate output products. The intermediate products are then combined through additional processing algorithms to eventually derive the final daily ET product. This paper will describe some of the uncertainties introduced by sensitivity of the SEBS model to a) land surface temperature and air
20 temperature gradient, b) the choice of fractional vegetation formula, c) displacement height and the height at which wind speed is measured, and d) study area heterogeneity.

2 Study area

The study area, situated in the Piketberg region in the Western Cape Province of South
25 Africa (Fig. 1), encompasses a quaternary catchment (G10K) in which commercial agriculture plays an important role. The area experiences winter rainfall (May to October), has a diverse topography and is drained by the perennial Berg River which enters the

Atlantic Ocean at Velddrif on the West Coast.

The climate in the area is varied with the western part of the catchment experiencing a maritime Mediterranean climate whilst the eastern part is considered to have a continental influence. The varying climate has an influence on the land use in the area with low-lying areas being dominated by dryland agriculture (predominantly wheat fields). In addition, temporary commercial irrigated agriculture (potatoes) under centre pivot irrigation as well as pockets of natural vegetation, described as shrublands and low fynbos, are found. The elevated area towards the northeast of the catchment is dominated by natural vegetation in the form of low- and high-fynbos with reported alien vegetation infestations. Cultivated irrigated lands in the form of deciduous and citrus fruit tree orchards are also found, although to a lesser extent.

2.1 Field validation site

Energy balance and evapotranspiration field measurements by Jarmain and Mengistu (2009) in an apple orchard on Moutons Valley farm from 7 November to 1 December 2008 were used to validate the results. Jarmain and Mengistu (2009) used a one-sensor Eddy covariance system for the estimation of the sensible heat flux density. The instrumentation was installed in the middle of the apple orchard in a section planted with Royal Gala trees. An RM Young three-dimensional ultrasonic anemometer (model 81000, Traverse city, Michigan, USA – path length of 150 mm) was used to estimate sensible heat flux density. Two net radiometers were used to measure the net radiation above the apple orchard. One REBS Q*6 net radiometer was installed above the apple tree row, and one NR-Lite net radiometer (Model 240-110, Kipp and Zonen) was installed above the inter-row area. The average value of these two sensors was used in the calculations. Soil temperature (using type-E soil averaging thermocouples) and soil heat fluxes (REBS heat flux plates) were measured at four different positions between the tree rows and the data was used to estimate the soil heat flux density. Using the estimates of sensible heat flux density and that of net irradiance and soil heat flux density, the latent energy flux density was subsequently calculated using the shortened

Full Screen / Esc

Printer-friendly Version

Interactive Discussion

energy balance equation (Jarmain and Mengistu, 2009).

At the time of the energy balance and total evaporation measurements in November 2008, the average canopy height was 3.2 m. The apple trees did not cover the soil surface completely, rather by about 75% and the inter-row areas were planted with grass (Jarmain and Mengistu, 2009).

Due to limited financial resources, field validation could not be conducted at multiple sites or for the entire hydrological year for which the water balance components were calculated. Therefore energy flux results presented in this research correspond to the specific field validation site and period. In addition, an automatic weather station installed in a wheat growing area (Piketberg: Pools-Ideal Hill) was used to compare results between land covers. However, there was no validation data available for this site.

3 Materials and methods

The Surface Energy Balance System (SEBS) is a scale-independent model proposed by Su (2002) for the estimation of atmospheric turbulent fluxes and evaporative fraction using satellite earth observation data in combination with meteorological information.

The SEBS model was used to estimate daily actual ET from remotely sensed and meteorological data by calculating the energy required for water to change phase from liquid to gas:

$$\lambda E = R_n - G - H \tag{1}$$

where λE is the turbulent latent heat flux (λ is the latent heat of vaporization and E is water vapour flux density), R_n is net radiation, G is the soil heat flux and H is the sensible heat flux (Su, 2002).

Reflectance and radiance measured by the satellite are used to calculate land surface parameters – albedo, emissivity, land surface temperature, NDVI and

fractional vegetation cover. The meteorological inputs required are radiation[1] ($W\,m^{-2}$), temperature[1,2] (°C), air pressure[1] (Pa) at surface and at reference height, specific humidity[1] ($kg\,kg^{-1}$) wind speed[1] ($m\,s^{-1}$) at reference height and sunshine duration[2] (h).

5   A simplified sequence illustrating the processing in SEBS is given in Table 1.

For the purpose of calculating ET in this research, MODIS (TERRA and AQUA) data were used. MODIS images are captured daily or every second day and therefore it is possible, in South Africa, to obtain a good coverage throughout the year. MOD02 and MYD02 data were selected for the field validation period.

10   The required meteorological data (air temperature, wind speed, radiation, sunshine duration) can be obtained directly from an automatic weather station (AWS) or indirectly (air pressure, specific humidity) using empirical formulae and data from the AWS. Weather data from the Mouton's Valley and the ARC-ISCW, Piketberg: Pools-Ideal Hill AWSs were used.

15   The SEBS model used for the research is available as part of the open source freeware ILWIS (available at: http://www.52north.org), making it a good choice to use for research purposes as researchers may use the already programmed model.

4   Uncertainties in evapotranspiration estimates with SEBS

The analysis of remote sensing and GIS products usually results in maps of discrete
20 or continuous variables (Dungan et al., 2002), which can be associated with several sources of error or uncertainty. These include: (1) errors or uncertainties associated with the specific remote sensing data obtained; (2) errors or uncertainties introduced with the processing and analysis of image and field data; (3) errors or uncertainties associated with the specific model; and (4) errors or uncertainties associated with

---

[1]Instantaneous, i.e. hourly average at time of satellite overpass

[2]Daily average

positional aspects (including image resolution). Wang et al. (2005) identify additional sources of errors including sampling and measurement error of ground truth data, errors of spectral values and radiometric calibration of images, errors from the leap from spectral measurements to interpretation of a categorical variable, modelling errors due to misunderstanding the relationship between spectral and thematic variables, and errors from GIS operations.

Uncertainties in the derivation of ET for this study were identified as (but are by no means limited to): (1) land surface and air temperature gradient; (2) the choice of fractional vegetation cover formula; (3) displacement height and the height of wind speed measurement in relation to displacement height; and (4) study area heterogeneity.

4.1 Land surface and air temperature gradient

The calculation of ET using the SEBS model relies on two temperature inputs: air temperature (T_a) and land surface temperature (T_0). Su (2002) reported on the sensitivity of sensible heat flux to the gradient of temperature change from land surface temperature to air temperature and Badola (2009) reported that of all remotely sensed input parameters, SEBS was most sensitive to change in ($T_0 - T_a$). T_0 plays a role in the determination of net radiation (R_n) (Table 1) and therefore soil heat flux (G_0), but its main contribution is in the calculation of aerodynamic resistance in the estimation of the sensible heat flux.

To quantify the uncertainty associated with T_0 estimates for the field validation site, the T_0 retrieved from MODIS data was compared with the Meteosat SEVIRI T_0 data product corresponding to the same time of image acquisition. It was found that there were differences of up to 10 K between MODIS T_0 and SEVIRI T_0 with SEVIRI T_0 being consistently higher than MODIS T_0 which is in agreement with the findings by Madeira et al. (2005). This high degree of uncertainty in T_0 can be ascribed to the topographically rough nature of the terrain in the vicinity of the field validation site.

In addition to the SEBS model sensitivity to T_0, the near-surface air temperature (T_a, as measured by weather stations) has a direct influence on the evaporation process

Full Screen / Esc

Printer-friendly Version

Interactive Discussion

and inaccuracies in measurements can lead to distorted reference ET measurements and actual ET estimates. For this reason, accuracy in air temperature measurements is needed at the weather stations themselves. Additionally, the heterogeneity of the study area (which will be described in Sect. 4.4) implies that an accurate interpola-
5 tion of air temperature across the study area is needed in the absence of distributed field-based air temperature measurements. This is because the spatial variations of surface characteristics (including topography and land cover) have a large influence on the near-surface weather conditions (Voogt, 2006). Increasing the accuracy of air temperature measurements and interpolation algorithms will increase the likelihood of
10 accurate ET estimates.

The sensitivity of daily ET calculated by SEBS to $\Delta (T_0 - T_a)$ for the field validation site was modelled by varying T_0 by up to 10 K around the estimated T_0 and keeping the T_a constant. The results (Fig. 2) indicated that for the apple orchard (where the estimated T_0 is 301 K, the estimated T_a is 293 K and $(T_0 - T_a)$ equals 8 K), daily ET can vary by up
15 to 1.5 mm in this 10 K $\Delta (T_0 - T_a)$ range. Adjusting T_a around a 10 K range, to create the same $\Delta (T_0 - T_a)$ as when T_0 was adjusted, results in a very similar daily ET range.

The modelling of the sensitivity of ET to T_0 in a wheat growing environment at Piket-berg: Pools-Ideal Hill (where the estimated T_0 is 311 K, the measured T_a is 295 K and $(T_0 - T_a)$ is 16 K) is also shown in Fig. 2. It can be seen that the sensitivity of daily ET
20 to $\Delta(T_0 - T_a)$ is much greater than in the apple orchard with a range of 7 mm across the same $\Delta(T_0 - T_a)$ where T_0 is increased and decreased by 10 K.

It can therefore be said that the sensitivity of daily ET to $\Delta(T_0 - T_a)$ is dependent on the land cover being studied and may also be dependent on the calculated $(T_0 - T_a)$ itself. It should, however, be noted that the uncertainty related to T_0 in the wheat growing area
25 is almost certainly lower than the 10 K range found in the apple orchard (field validation site) since the wheat growing area is topographically flat and relatively homogeneous. This implies that it is unrealistic to expect the extreme uncertainty in daily ET as may be implied in Fig. 2. However, it is useful to note the differences in sensitivity to $\Delta(T_0 - T_a)$ on the same day, for two land covers in close proximity to each other, therefore re-

Title Page

Abstract | Introduction

Conclusions | References

Tables | Figures

⏮ | ⏭

◀ | ▶

Back | Close

Full Screen / Esc

Printer-friendly Version

Interactive Discussion

emphasizing the care (particularly to the accuracy of input data) that should be taken when using SEBS in a heterogeneous environment.

Furthermore, the calculated sensitivity of the sensible heat flux in the wheat growing area in this study to $\Delta(T_0-T_a)$, of $\Delta H=10.82\Delta(T_0-T_a)$ is in close agreement with the sensitivity of $\Delta H = 10\Delta(T_0-T_a)$ reported by Su (2002) for cotton. However, it was found that calculated sensitivity of the sensible heat flux to $\Delta(T_0-T_a)$, in this study, for the apple orchard, is of $\Delta H = -8.68\Delta (T_0-T_a)$ where T_0 was taken to be less than the estimated T_0 and of $\Delta H=6.17\Delta(T_0-T_a)$ where T_0 is taken to be greater than the estimated T_0. It can therefore be seen that the sensitivity of H (and therefore daily ET) to $\Delta(T_0-T_a)$ is dependent both on the land cover type and T_0 itself.

The uncertainties in the interpolation of T_a together with the uncertainties related to T_0 estimates create ambiguity with regard to the accuracy of the results. This is particularly prohibitive since these parameters are used in the initial stages of SEBS model implementation, meaning that erroneous input data would be translated through the entire processing sequence and eventually be reflected in the final calculation of actual ET.

4.2 Fractional vegetation cover

Fractional vegetation cover (fc) and its complement are used in the calculation of the roughness length for heat transfer (Su et al., 2005) which, in turn, is used in the calculation of the sensible heat flux. In addition, fc is used in the estimation of the soil heat flux (Su, 2002).

Several methods for the calculation of fc are described in the literature. These methods generally make use of leaf area index (LAI) (Choudhury, 1987, cited in French et al., 2003) as input or require pixel NDVI together with a minimum and maximum NDVI value (Carlson and Ripley, 1997; Gutman and Ignatov, 1998). These minimum and maximum NDVI values are either constant (Sobrino and El Kharraz, 2003) or can be derived directly from the scene or from a time series.

For example, if fractional vegetation cover is calculated according to the formula for vegetation proportion (Sobrino and El Kharraz, 2003):

$$fc = \frac{(NDVI - NDVI_{min})^2}{(NDVI_{max} - NDVI_{min})^2} \qquad (2)$$

where NDVImin is defined to be 0.2 and NDVImax is defined to be 0.5. In this application of the formula, pixels with NDVI values of 0.5 or higher are considered to be fully vegetated and pixels with values of 0.2 or lower are considered to be sparsely vegetated or to contain bare soil.

In contrast with $NDVI_{min}$ and $NDVI_{max}$ values as defined by Sobrino and El Kharraz (2003), Fig. 3 shows the distribution of NDVI values across the entire study area for a winter wet season and summer dry season scene. It can be seen that the range of 0.2 to 0.5 is frequently exceeded within this study area, particularly in the winter wet season. The distribution of NDVI in this study area is therefore scene and season dependent.

At a NDVI value of 0.5 and higher, maximum vegetation cover is assumed and fc=1. The assumption is therefore that the soil is completely shaded, and based on the soil heat flux equation (Su, 2002), the soil heat flux is only a function of net radiation and fractional vegetation cover, equaling 5% of net radiation. In contrast, the field valida-tion data (in the apple orchard) at TERRA overpass indicate a relatively high soil heat flux (approximately 12–16% of net radiation) since the bare soil underneath the trees receives direct radiation as a result of the solar zenith and azimuth angle in combina-tion with the orientation of the tree rows. At AQUA overpass, when the soil of the field validation site is shaded, there is a much better agreement between field validation (approximately 3–15% of net radiation) and the SEBS results (approximately 5% of net radiation) for soil heat flux.

The fractional vegetation cover calculation can be tested using the field validation data and by rearranging the soil heat flux equation (Su, 2002):

$$\text{fc} = -\left[\frac{\frac{G_0}{R_n} - \Gamma_c}{\Gamma_s - \Gamma_c}\right] - 1 \tag{3}$$

Solving Eq. (3) by substituting the field measured G_0 values, fractional vegetation cover is calculated to range from 0.58–0.73 at TERRA overpass and at AQUA overpass from 0.67–1. If this is taken to be a true reflection of fractional vegetation cover at image acquisition time, the NDVI minimum and maximum values should be adjusted as a fractional vegetation cover of 1 is not a realistic result especially at TERRA acquisition time.

Considering fc calculated above, the need for defining an appropriate NDVI_{max} for the study area is apparent. Substituting this fc and the corresponding NDVI for the field validation site for each MODIS TERRA and AQUA acquisition and keeping the $\text{NDVI}_{min}=0.2$ as suggested by Sobrino and El Kharraz (2003) in Eq. (2) results in an average $\text{NDVI}_{max}=0.65$, which is more appropriate for the study area during the field validation period. Using the newly defined NDVI_{max}, the calculated soil heat flux more closely approximates the field measured soil heat flux.

Furthermore, where fc=1, sensible heat flux is at a minimum and actual ET equals potential ET. This is the case where $\text{NDVI}_{max}=0.5$. However actual ET≠potential ET where $\text{NDVI}_{max}=0.65$.

The benefits of using a set minimum and maximum NDVI should be weighed up against using scene-specific estimates especially for scenes which do not contain a full range of vegetation cover as this will skew the results of the fractional vegetation calculation. The sensitivity of daily ET to choice of fc formula and selection method for NDVI_{min} and NDVI_{max} is shown in Fig. 4 for the apple orchard at the field validation site. It can be seen that in this instance, the calculated daily ET can vary by up to 0.7 mm depending on the fc input.

From the results it can be concluded that if it is possible to obtain field data in order to derive an appropriate NDVI minimum and maximum value, the formula by Carlson and Ripley (1997) can be used. Alternatively the formula by Choudhury (1987) cited in French et al. (2003) using LAI as input may be used as it gives the same result.

5 Fractional vegetation cover is calculated outside of SEBS and care should be taken in the choice of formula as the variation in ET as a function of fc has been demonstrated.

4.3 Displacement height

Displacement height (d_0) values are used in combination with the reference height at which wind speed is measured (z) in the process of determining the sensible heat 10 flux (H). d_0 can be obtained from the literature or can be empirically derived from the remote sensing vegetation inputs via the calculation of roughness length (the methodology adopted by Su, 2002; Timmermans et al., 2005; and Van der Kwast et al., 2009). Alternatively the combination approach of Jia et al. (2009) can be used. Using the empirical model, NDVI and $NDVI_{max}$ are used to determine roughness length for mo-15 mentum transfer (z_{0m}) with the method described by Su and Jacobs (2001) as reported in Hailegiorgis (2006). Next, the vegetation height is calculated from z_{0m} followed by d_0 using the method of Brutsaert (1982) as reported in Hailegiorgis (2006).

In South Africa, the installation of automatic agrometeorological weather stations complies with standards set by the World Meteorological Organisation except in the 20 height measurement of wind speed and direction. South African agrometeorological standards state that wind speed and wind direction are measured at 2 m above the surface (ARC-ISCW, 2010) in contrast to the South African Weather Service (SAWS) which measures wind speed and direction at 10 m above the surface.

A problem arises when using data from agrometeorological weather stations in 25 canopies of 3 m or higher (where $d_0 \geq 2$), as is the case with orchards in the study area. To derive the sensible heat flux (Su, 2002) the calculation of $z - d_0$ is required, where z is the reference height at which wind speed is measured (2 m, in the case of an agrometeorological weather station). When measuring wind speed at 2 m, and

solving for H using the equations defined by Su (2002), a situation arises where $z \leq d_0$, and the ln of a negative number needs to be solved.

In this study, the average canopy height at the field validation site was reported to be 3.2 m (Jarmain and Mengistu, 2009) and therefore $d_0 > 2$ m so the condition where $z \leq d_0$ is reached using agrometeorological weather stations. The alternative would be to use weather data from the SAWS which would allow for the sensible heat flux to be calculated for much higher canopies than for the above scenario. However, it is agrometeorological weather stations which are installed in agricultural areas where this and other studies of this nature take place. Should only agrometeorological weather station data be available, the upscaling of the available meteorological data to a higher reference height should be investigated based on radiosonde observations (Ershadi, 2010).

The effect on d_0 in high canopies is shown by using the field validation site as an example, and testing for the sensitivity of daily ET to d_0 (Fig. 5) At approximately $d_0 = 1.8$ m, a rapid decrease in daily ET estimation is noted as d_0 approaches 2 m. It can be surmised therefore (although this should be tested in different environments and under different meteorological conditions) that when using wind speed measured at 2 m above the surface, the SEBS model should not be used in canopies of 2.7 m and higher as it is at this point that the model becomes highly sensitive to changes in d_0.

The uncertainty in the calculation of the sensible heat flux introduced by uncertainties in displacement height and the height of wind speed measurement should be carefully considered and addressed since errors in the calculation of the sensible heat flux will be propagated through the model and eventually influence the final ET calculation.

4.4 Heterogeneity of the study area

Heterogeneity as related to the concept of the spatial variability of a landscape plays an important role in the application of remote sensing data to the calculation of ET, especially in the selection of the spatial resolution of the particular sensor. Various studies have shown that, for complex heterogeneous landscapes, there is lower confidence in

variables derived using low resolution sensor data (Garrigues et al., 2006; Kustas et al., 2004; Lakhankar et al., 2009; Li et al., 2006; Li et al., 2008; McCabe and Wood, 2006; Moran et al., 1997) as intra-pixel spatial heterogeneity is lost due to the integration of the radiometric signal.

5   Land cover (mapped at 1:50 000 scale) and topography data (elevation from SRTM at 90 m resolution) are used to demonstrate the heterogeneity of the study area. Sub-pixel variability of elevation (as a proxy for topography) and land cover are estimated within the MODIS pixel (1 km resolution). For land cover, the frequency distribution of particular land cover classes (natural and cultivated) within the 1 km pixel is used to
10   reveal the degree of heterogeneity (Fig. 6). Dryland agriculture appears as the most homogeneous land cover class with commercially irrigated classes being the most heterogeneous (including orchards).

      The effect of landscape heterogeneity on variables (including SEBS input parameters) derived from MODIS is illustrated using NDVI by way of example. Figure 7 shows
15   the variability of NDVI per land cover class as measured by the standard deviation of NDVI values at 1 km resolution. The mixed pixel effect shown for land cover classes covering less than 40–50% can be clearly seen by the variability of the NDVI. At higher percentages, NDVI values are less variable indicating higher confidence in NDVI values in more homogeneous areas.

20   In addition to the direct effect of landscape heterogeneity and spatial resolution of input data on remote sensing variables illustrated above, landscape heterogeneity can also indirectly affect spatial modelling efforts. As an example, the topographic effects on near-surface meteorological conditions are considered. Spatial variations of surface characteristics, especially surface topography, have a large influence on the near-
25   surface weather conditions (ARC-ISCW, 2010). The heterogeneity of the surface elevation as a proxy for variable topography can be seen from Fig. 8 which shows the coefficient of variation of elevation within each land cover class. The variation of elevation within land cover is most pronounced in the land cover classes containing dryland agriculture and low fynbos. The commercially irrigated classes show the least variability in

elevation as expected since the topography is one of the variables that determines the suitability of an area for irrigated agriculture on a commercial scale.

Figure 9 illustrates the sub-pixel variation of elevation within the coarser 1 km pixel. The standard deviation increases with the mean up to elevation values of 500 m with a scattered pattern at higher elevations. The relative variability as measured by the coefficient of variation varies significantly at elevations lower than 250 m and decreases with the increase in elevation values.

The topographic heterogeneity illustrated above implies that spatially distributed measurements of near-surface weather conditions would ideally be needed for accurate retrieval of parameters needed for ET calculation. However, in the absence of distributed measurements an accurate interpolation algorithm considering the variability in topography could be applied to alleviate at least some of the uncertainty.

5 Discussion

The complexities associated with the derivation of ET and the uncertainties described in Sect. 4 imply that potential errors will be introduced at various stages of ET derivation. These errors are related to error production and error propagation as defined by Veregin (1989). Error production refers to a situation where errors in output products are attributed mainly to the specific operations applied to the data, thereby producing errors in the output products while no errors were present in the original data used as input. On the other hand, error propagation refers to the process where potentially erroneous input data is passed through certain processing sequences and errors accumulate in output products. In the case of deriving ET, errors will be compounded if intermediate error-bearing output products are used in additional processing sequenced to derive the final result.

The opportunity for error production is introduced when it is considered that the SEBS model is complex in itself as it consists of three tools (Su, 2006), namely:

– a set of tools to determine physical parameters of the land surface;

– an extended model to derive roughness length for heat transfer; and

– a model to determine evaporative fraction on the basis of energy balance.

An example of error production was illustrated in the case of deriving fractional vegetation cover using ill-defined NDVI limits. An error in the calculation of fractional vegetation cover would be propagated to soil and sensible heat flux calculations. This in turn will be propagated to the calculation of the latent heat flux and therefore ET. Prior to adjusting $NDVI_{max}$ for the study area, ET was calculated to equal reference ET. After adjusting $NDVI_{max}$ ET was no longer calculated to be equal to reference ET in better agreement with field validation results. In the absence of known suitable NDVI maximum and minimum values a priori, then a fractional vegetation cover formula, such as proposed by Choudhury (1987) cited by French et al. (2003), which makes use of LAI rather than NDVI may be used.

The opportunity for error propagation is introduced at the initial stages of ET derivation when it is considered that remote sensing data together with standard meteorological data are required by the SEBS model. Due to uncertainties associated with remote sensing and the interpolation of meteorological data, potential errors will propagate throughout the processing sequence.

An opportunity for error propagation is introduced when considering land surface temperature, air temperature and their gradient ($T_0 - T_a$) since T_0 values derived from two different sources differed by up to 10 K for the field validation site. The sensitivity of SEBS to ($T_0 - T_a$) appears to vary between land covers and the sensitivity may be dependent on the estimated T_0 value itself. This implies that a small error in the input data would propagate through the model and cause large uncertainty in the final derivation of ET. However, the range in uncertainty cannot be modelled as it appears to vary between land cover types. Furthermore, the use of air temperature from weather stations interpolated across a study area introduces more opportunities for error propagation, especially in a heterogeneous environment where T_a may vary over a short distance dependent on inter alia land cover. This will be compounded in areas with

limited weather station coverage in a heterogeneous environment due to the influence of topography on near-surface weather conditions.

From the data presented here it can be seen that the study area comprises a spatially diverse landscape with a high level of heterogeneity. In order to successfully estimate ET and capture the full range of variability in fluxes, the choice of spatial resolution of remote sensing data is crucial. Kustas et al. (2004) and Li et al. (2006) found that when the spatial resolution exceeds 500 m, mixed pixels containing large contrasts in surface temperature and vegetation cover could cause significant errors (Li et al., 2008). Flores et al. (2009) also demonstrated the impact of topographic heterogeneity on near-surface soil temperature. Although it has been found that MODIS has limited capacity in capturing the spatial variability in fluxes at field level, estimates for the spatial average flux at large scales may be accurate (McCabe and Wood, 2006). However, in addition to this, the accurate interpolation of meteorological data across a heterogeneous study is vital as model sensitivity to $(T_0 - T_a)$ has been shown.

It is recognised that errors produced or propagated through complex models would need to be assessed, modelled and accurately documented in order to lend credibility to final results in this particular study area.

6 Concluding remarks

The overall objective of this project was to determine the usefulness and applicability of using remote sensing technologies as a tool for resource assessment and determination of water use. Although promising, uncertainties in estimating the various parameters were encountered. These uncertainties could broadly be classified as 1) errors in input data, 2) uncertainties related to spatial heterogeneity of the study area and resolution of input data, and 3) processing errors resulting in either error production or error propagation or both.

This paper described some of these uncertainties by example of the derivation of evapotranspiration using the SEBS model. Uncertainty related to input data was

demonstrated through investigating problems related to land surface and air temperature as well as in the derivation of displacement height. Uncertainty related to the heterogeneity of the study area in terms of land cover and topography in relation to the spatial resolution of input data was also demonstrated. Finally, uncertainty in data pro-
5 cessing was demonstrated using the case of determining fractional vegetation cover as example. These uncertainties and potential errors are compounded when considering that the SEBS model for calculating ET is a complex process, requiring several image processing sequences that are combined to produce the final result. This may lead to a situation where errors may be propagated and compounded through the processing
10 chain, eventually affecting the final output product.

The various uncertainties and potential errors of propagation and production mean that great uncertainty is associated with the accuracy of the final output product. Ideally, sources of uncertainty will need to be identified and the accumulation and propagation of errors will need to be modelled. This will enable the quantification of error or
15 uncertainty originating either from source data or through processing errors.

Simultaneous multi-parameter sensitivity analysis of inputs which are used in the SEBS model would help in determining to which parameters the SEBS model is most sensitive and under which conditions these sensitivities are the most pronounced. This would begin to address the uncertainties highlighted in this research and may lead to
20 greater confidence in using SEBS generated ET results.

Although illustrating uncertainty using ET as an example, the derivation of all the components of the water balance equation using remote sensing data were influenced by similar uncertainties and the actual water consumption of individual agricultural fields could not be calculated. However, methodologies untested in South Africa were
25 applied to the study area with many challenges encountered at both a data and skills capacity level. If the uncertainties and limitations encountered in the course of the research project are considered and acted upon it may be possible that at least parts of the methodology may be relevant at a later stage for water use determination.

Discussion Paper | Discussion Paper | Discussion Paper | Discussion Paper

References

ARC-ISCW: Technical manual for the AgroClimatology Weather Station Network. ARC-ISCW internal report, Agricultural Research Council-Institute for Soil, Climate and Water, South Africa, Report No. GW/A/2008/60, 2010.
10 Badola, A.: Validation of Surface Energy Balance System (SEBS) over forest land cover and sensitivity analysis of the model, M.Sc. thesis, International Institute for Geo-information Science and Earth Observation, The Netherlands, 2009.
Carlson, T. N. and Ripley, D. A.: On the relation between NDVI, fractional vegetation cover, and leaf area index, Remote Sens. Environ., 62, 241–252, 1997.
15 Dungan, J. L., Kao, D., and Pang, A.: The uncertainty visualization problem in remote sensing analysis, in: Proceedings of Int. Geosci. Remote Se., Toronto, Canada, June 2, 2002, 729–731, 2002.
Ershadi, A.: Land-atmosphere interactions from canopy to troposphere, M.Sc. thesis, International Institute for Geo-information Science and Earth Observation, The Netherlands, 2010.
20 Flores, A. N., Ivanov, V. Y., Entekhabi, D., and Bras, R. L.: Impact of hillslope-scale organization of topography, soil moisture, soil temperature, and vegetation on modelling surface microwave radiation emission, IEEE T. Geosci. Remote, 47, 2557–2571, 2009.
French, A. N., Schmugge, T. J., Kustas, W. P., Brubaker, K. L., and Prueger, J.: Surface energy fluxes over El Reno, Oklahoma, using high-resolution remotely sensed data, Water Resour.
25 Res., 39, 1164, doi:10.1029/2002WR001734, 2003.
Garrigues, S., Allard, D., Baret, F., and Weiss, M.: Quantifying spatial heterogeneity at the landscape scale using variogram models, Remote Sens. Environ., 103, 81–96, 2006.
Gibson, L. A., Munch, Z., Engelbrecht, J., Petersen, N., and Conrad, J. E.: Remote sensing as a tool for resources assessment towards the determination of the legal compliance of

Title Page

Abstract | Introduction

Conclusions | References

Tables | Figures

◄ | ►►

◄ | ►

Back | Close

Full Screen / Esc

Printer-friendly Version

Interactive Discussion

surface and groundwater use, Water Research Commission, Pretoria, South Africa, WRC Report No. 1690/1/09, 2010.

Gutman, G. and Ignatov, A.: The derivation of the green vegetation fraction from NOAA/AVHRR data for use in numerical weather prediction models, Int. J. Remote Sens., 19, 1533–1543, 1998.

Hailegiorgis, W. S.: Remote sensing analysis of summer time evapotranspiration using SEBS algorithm: a case study in Regge and Dinklel, The Netherlands, M.Sc. thesis, International Institute for Geo-information Science and Earth Observation, The Netherlands, 2006.

Jarmain, C. and Mengistu, M. G.: Validating energy fluxes estimated using the surface energy balance system (SEBS) model for a small catchment, Water Research Commission, Pretoria, South Africa, Consultancy Report No. K8/824, 2009.

Jia, L., Xi, G., Liu, S., Huang, C., Yan, Y., and Liu, G.: Regional estimation of daily to annual regional evapotranspiration with MODIS data in the Yellow River Delta wetland, Hydrol. Earth Syst. Sci., 13, 1775–1787, doi:10.5194/hess-13-1775-2009, 2009.

Kustas, W. P., Li, F., Jackson, T. J., Prueger, J. H., MacPherson, J. I., and Wolde, M.: Effects of remote sensing pixel resolution on modelled energy flux variability of croplands in Iowa, Remote Sens. Environ., 92, 535–547, 2004.

Lakhankar, T., Ghedira, H., Temimi, M., Azar, A. E., and Khanbilvardi, R.: Effect of land cover heterogeneity on soil moisture retrieval using active microwave remote sensing data, Remote Sens., 1, 80–91, doi:10.3390/rs1020080, 2009.

Li, Z., Yu, G., Li, Q., Fu, Y., and Li, Y.: Effect of spatial variation on areal evapotranspiration simulation in Haibei, Tibet plateau, China, Int. J. Remote Sens., 27, 3487–3498, 2006.

Li, F., Kustas, W. P., Anderson, M. C., Prueger, J. H., and Scott, R. L.: Effect of remote sensing spatial resolution on interpreting tower-based flux observations, Remote Sens. Environ., 112, 337–349, 2008.

Madeira, C., Dash, P., Olesen, F., and Trigo, I.: Intercomparison of Meteosat-8 derived LST with MODIS and AATSR similar products, in: Proceedings of the 2005 EUMETSAT Meteorological Satellite Conference, Dubrovnik, Croatia, 19–23 September 2005, available at: http://www.eumetsat.int/Home/Main/AboutEUMETSAT/Publications/ConferenceandWorkshopProceedings/2005/SP_1232458833219?l=en, 2005.

McCabe, M. F. and Wood, E. F.: Scale influences on the remote estimation of evapotranspiration using multiple satellite sensors, Remote Sens. Environ., 105, 271–285, 2006.

Moran, M.S, Humes, K. S., and Pinter Jr., P. J.: The scaling characteristics of remotely-

Title Page

Abstract | Introduction

Conclusions | References

Tables | Figures

◀ | ▶

◀ | ▶

Back | Close

Full Screen / Esc

Printer-friendly Version

Interactive Discussion

sensed variables for sparsely-vegetated heterogeneous landscapes, J. Hydrol., 190, 337–362, 1997.

Sobrino, J. A. and El Kharraz, J.: Surface temperature and water vapour retrieval from MODIS data, Int. J. Remote Sens., 24, 5161–5182, 2003.

5 Su, Z.: The Surface Energy Balance System (SEBS) for estimation of turbulent heat fluxes, Hydrol. Earth Syst. Sci., 6, 85–100, doi:10.5194/hess-6-85-2002, 2002.

Su, Z.: An introduction to the surface energy balance system (SEBS), Lecture notes, ESA TIGER Capacity Building Facility 1st Training Course on "Advanced optical remote sensing", Cape Town, 22–25 November 2006, 2006.

10 Su, H., McCabe, M. F., and Wood, E. F.: Modeling evapotranspiration during SMACEX: comparing two approaches for local- and regional-scale prediction, J. Hydrometeorol., 6, 910–922, 2005.

Su, Z., Wang, L., and Parodi, G. N.: SEBS for ILWIS Open Source: A Practical Tool for Surface Energy Balance Estimates from Remote Sensing Data, Surface Energy Balance Models of

15 Agricultural Areas from Earth Observation Data, Lima, Perú, 13 March 2008, 2008.

Timmermans, W. J., van der Kwast, J., Gieske, A. S. M., Su, Z., Olioso, A., Jia, L., and Elbers, J.: Intercomparison of energy flux models using ASTER imagery at the SPARC 2004 site, Barrax, Spain, in: Proceedings of the ESA WPP-250: SPARC final workshop, Enschede, 4–5 July 2005, p. 8, 2005.

20 van der Kwast, J., Timmermans, W., Gieske, A., Su, Z., Olioso, A., Jia, L., Elbers, J., Karssenberg, D., and de Jong, S.: Evaluation of the Surface Energy Balance System (SEBS) applied to ASTER imagery with flux-measurements at the SPARC 2004 site (Barrax, Spain), Hydrol. Earth Syst. Sci., 13, 1337–1347, doi:10.5194/hess-13-1337-2009, 2009.

Veregin, H.: Error modelling for the map overlay operation, in: Accuracy of Spatial Databases,

25 edited by: Goodchild, M. F. and Gopal, S., Taylor and Francis, London, 3–18, 1989.

Voogt, M. P.: Meteolook, a physically based regional distribution model for measured meteorological variables. M.Sc. Thesis TU Delft, abstract available at: http://www.citg.tudelft.nl/live/pagina.jsp?id=50e40a94-07c2-4ccc-a3e9-849c85ecbfd0&lang=en&binary=/doc/Voogt2006.pdf, 2006.

30 Wang, G., Gerther, G. Z., Fang, S. and Anderson, A. B.: A methodology for spatial uncertainty analysis of remote sensing and GIS products, Photogramm. Eng. Rem. S., 17, 1423–1432, 2005.

Title Page

Abstract | Introduction

Conclusions | References

Tables | Figures

|◄ | ►|

◄ | ►

Back | Close

Full Screen / Esc

Printer-friendly Version

Interactive Discussion

Table 1. Sequence of SEBS processing (adapted from Su et al., 2008).

Inputs		Outputs
Incoming shortwave radiation (SW↓), land surface temperature (T_0), albedo (α), air temperature (T_a), land surface emissivity (ε_a)	→	Net radiation (R_n)
Fractional vegetation cover (fc), α, R_n	→	Land surface emissivity (ε_a), Soil heat flux (G_0) Sensible heat flux (H_{dry})
R_n, G_0	→	Sensible heat at the dry limit (H_{dry})
Horizontal wind speed (U), T_0, T_a, Leaf Area Index (LAI), Roughness length for momentum transfer (Z_{om}), fc	→	Frictional velocity (u^*), Monin-Obukhov length (L), Sensible heat flux (H), Excess resistance to heat transfer (kB^{-1}), Roughness length for heat transfer (Z_{oh})
Specific humidity (es), R_n, G_0, u^*, Z_{oh}	→	Wet-limit stability length (L_{wet}), Sensible heat flux at the wet limit (H_{wet})
H_{dry}, H_{wet}, H	→	Relative evaporation (Λr)
H_{wet}, R_n, G_0	→	Evaporation at the wet limit (λE_{wet})
λE_{wet}, Λr, R_n, G_0	→	Evaporative fraction (Λ)
Λ, Daily radiation (R_{n24}), Daily soil heat flux (G_{24})	→	E_{daily}
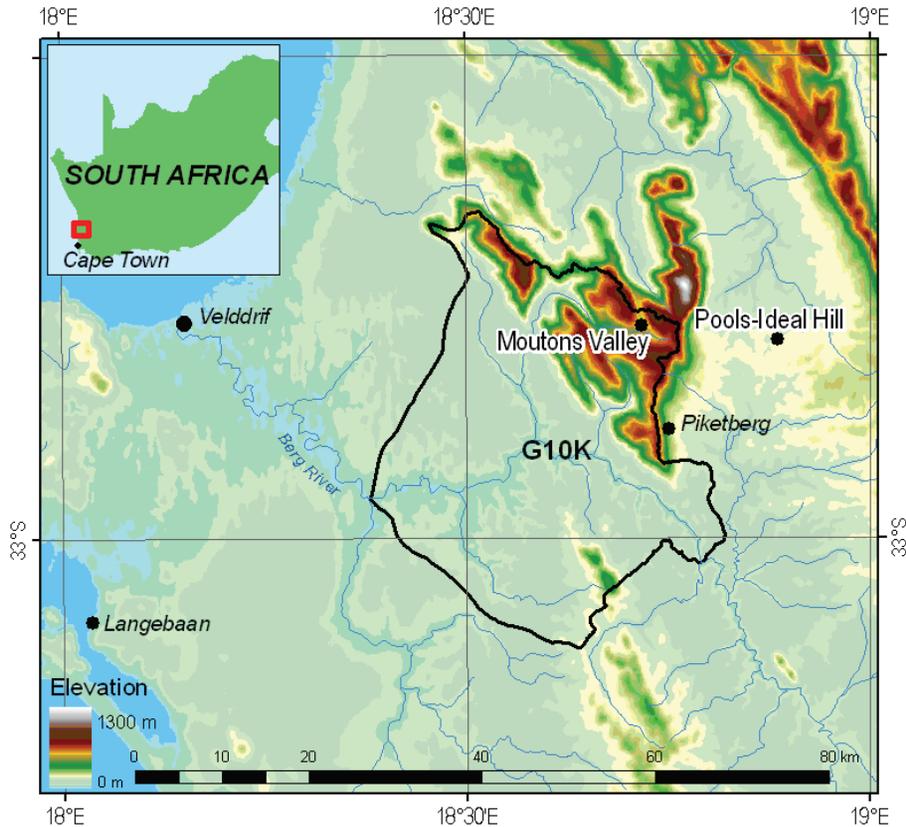
Fig. 1. Orientation map showing the G10K catchment, the field validation site (Mouton's Valley) and the weather station (Pools-Ideal Hill) situated in a wheat growing area which was used for experimental purposes.
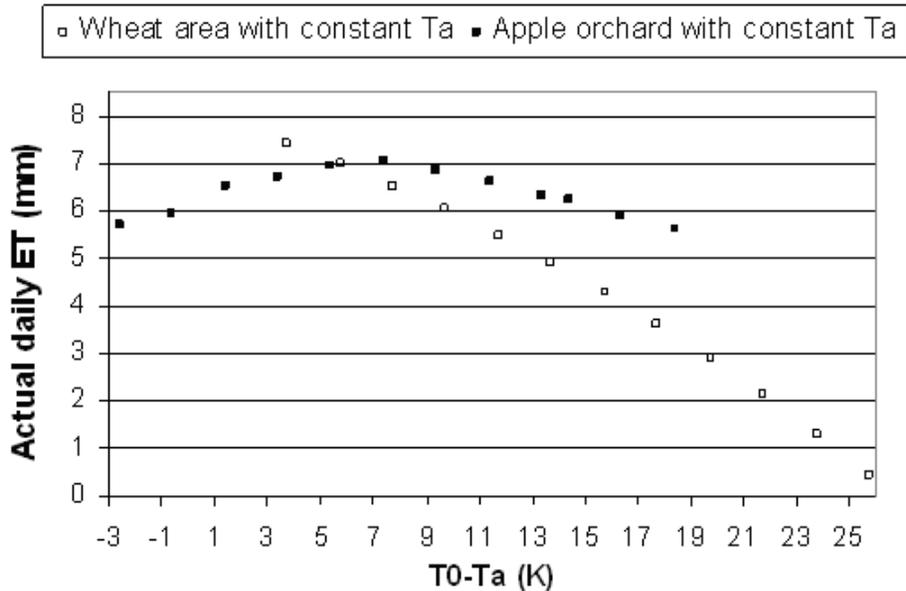
Fig. 2. Sensitivity of SEBS-estimated daily ET to $\Delta(T_0 - T_a)$ for an apple orchard and a wheat growing area.
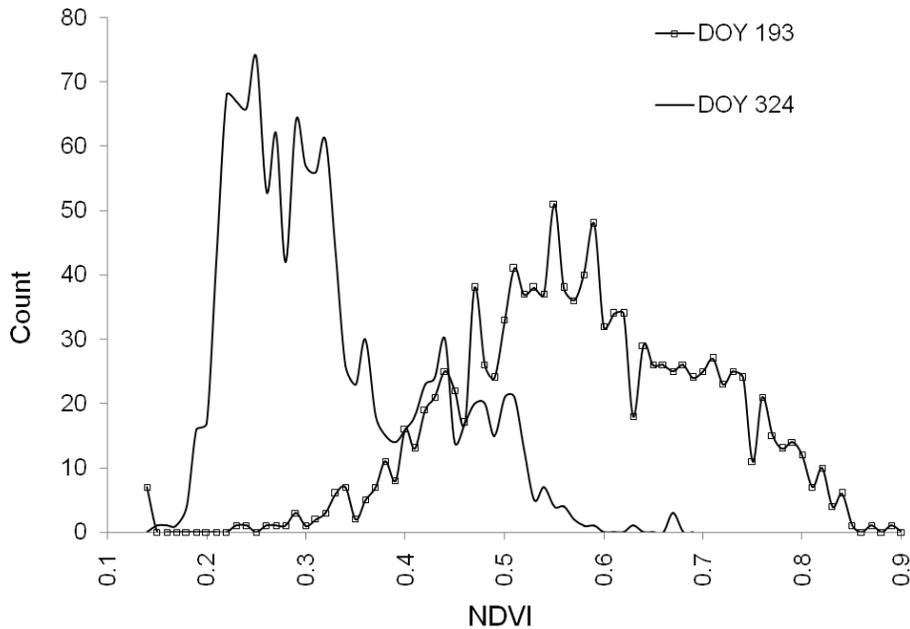
Fig. 3. NDVI distribution for the study area for a winter scene (DOY 193) and a summer scene (DOY 324).

Full Screen / Esc

Printer-friendly Version

Interactive Discussion
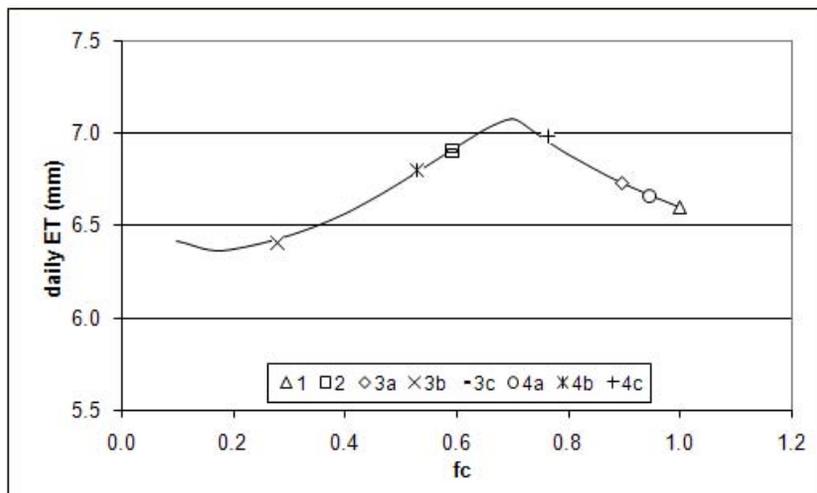
1	Fixed NDVI max (0.5) and min (0.2) (Sobrino & El Kharraz, 2003))
2	LAI dependent (Choudhury, 1987, cited in French et al., 2003)
3a	Scene dependent NDVI max (0.563) and min (0.207) (Carlson & Ripley, 1997)
3b	Time series derived NDVI max (0.863) and min (0.184) (Carlson & Ripley, 1997)
3c	Study area derived NDVI max (0.65) and min (0.2) (Carlson & Ripley, 1997)
4a	Scene dependent NDVI max (0.563) and min (0.207) (Gutman & Ignatov, 1998)
4b	Time series derived NDVI max (0.863) and min (0.184) (Gutman & Ignatov, 1998)
4c	Study area derived NDVI max (0.65) and min (0.2) (Gutman & Ignatov, 1998)

Note: where fc is calculated to be greater than 1, then fc is taken to be equal to 1

Fig. 4. Sensitivity of SEBS-estimated ET to a range in fractional vegetation cover input values for the apple orchard field validation site. fc values resulting from specific formulae and methods are indicated.
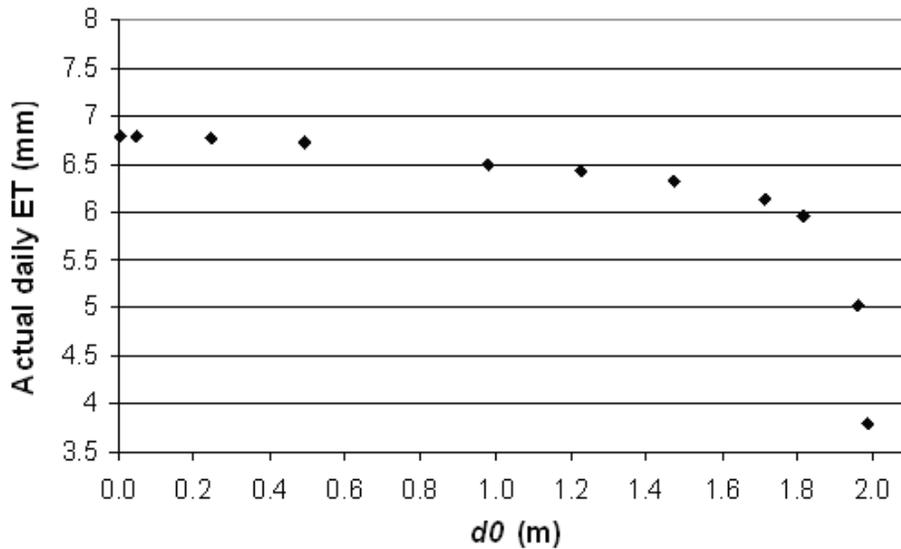
Fig. 5. Sensitivity of SEBS-estimated ET to d_0 for the apple orchard field validation site when wind speed is measured at 2 m.

Fig. 6. Histogram of sub-pixel heterogeneity of land cover type within MODIS pixel (1 km).
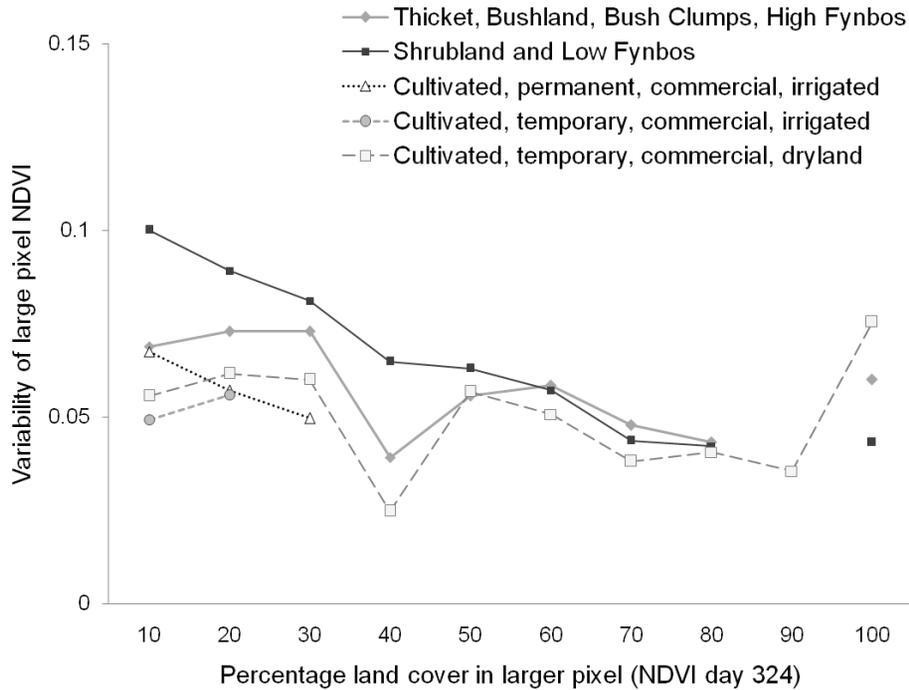
Fig. 7. Variability of NDVI in 1 km pixel measured by standard deviation for land cover classes.
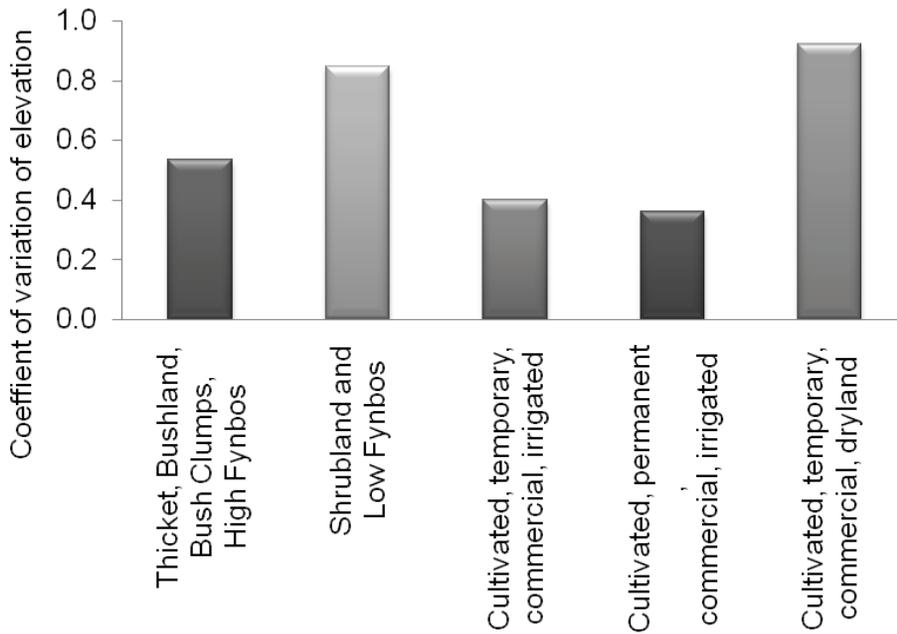
Fig. 8. Heterogeneity in topography as a function of land cover.

Title Page

Abstract | Introduction

Conclusions | References

Tables | Figures

|◄ | ►|

◄ | ►

Back | Close

Full Screen / Esc

Printer-friendly Version

Interactive Discussion
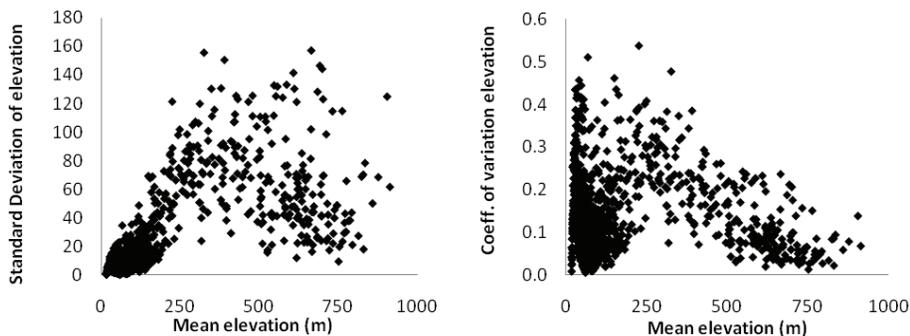
Fig. 9. Relationship of mean elevation to variability illustrating heterogeneity in topography.